Journal of Mechanics Engineering and Automation 2 (2012) 555-562

Lateral Stability Improvement of Car-Trailer Systems Using Active Trailer Braking Control

Tao Sun, Yuping He, Ebrahim Esmailzadeh and Jing Ren

Faculty of Engineering and Applied Science, University of Ontario Institute of Technology, Oshawa, Ontario L1H 7K4, Canada

Received: July 04, 2012 / Accepted: August 01, 2012 / Published: September 25, 2012.

Abstract: An active trailer braking controller to improve the lateral stability of car-trailer systems is presented. The special and complex structures of these types of vehicles exhibit unique unstable motion behavior, such as the trailer swing, jack-knifing and rollover. These unstable motion modes may lead to fatal accidents. The effects of passive mechanical parameters on the stability of car-trailer systems have been thoroughly investigated. Some of the passive parameters, such as the center of gravity of the trailer, may be drastically varied during various operating conditions. Even for an optimal design of a car-trailer system, based on a specific passive parameter set, the lateral stability cannot be guaranteed. In order to improve the lateral stability of car-trailer systems, an active trailer braking controller is designed using the Linear Quadratic Regular (LQR) technique. To derive the controller, a vehicle model with 3 Degrees Of Freedom (DOF) is developed to represent the car-trailer system. A single lane-change maneuver has been simulated to examine the performance of the controller and the numerical results are compared with those of the baseline design. The benchmark investigation indicates that the optimal controller based on the LQR technique can effectively improve the high-speed lateral stability of the car-trailer system.

Key words: Car-trailer systems, active trailer braking control, LQR (linear quadratic regular) controller, high-speed lateral stability.

1. Introduction

A car-trailer system generally consists of a powered unit, such as a SUV or passenger car, and one towed unit, called trailer. Individual units are connected to one another at an articulated point by a hitch. In North America, car-trailer systems are widely used to transport goods and materials due to their cost-effectiveness and versatility [1].

However, due to complex structures of car-trailer systems, they have unique unstable motion modes which include the trailer swing, jack-knifing, and rollover [2]. Jack-knifing is one of the most common causes for serious traffic accidents, in which car/trailer are involved. It is mainly attributed to tire/ground friction force saturation that may occur in curved path negotiations or during heavy braking processes. If the articulation angle between the leading and trailing units exceeds a critical limit, the driver is unable to control the motion of the vehicle system by steering. Similar to the jack-knifing, the trailer swing is also a yaw instability mode in term of divergent trailer yaw response. The rollover of car-trailer system is another dangerous safety problem worldwide.

Three major factors contributing to rollover accidents are: (1) high-speed curved path negotiations, such as a car-trailer system operating at high merging speeds on highway ramps; (2) sudden course deviation from high initial speed, e.g., lane-change maneuvers; and (3) load shift. The rollover stability is limited by the vehicle’s static rollover threshold expressed as the lateral acceleration in gravitational units (g). Single unit cars’ rollover thresholds are higher than 1 g, while the threshold of a car-trailer system may be as

Tao Sun, master’s student, research fields: vehicle system dynamics, active safety systems.

Corresponding author: Yuping He, Ph.D., associate professor, research fields: vehicle system dynamics, design optimization, modeling and simulation, driver-in-the-loop real-time simulation. E-mail: yuping.he@uoit.ca.

low as 0.6 g [3]. These unstable motion modes may lead to fatal accidents.

To date, the majority of car-trailer systems employ passive mechanisms to enhance the high-speed lateral stability. The Hensley Arrow uses a series of mechanical linkages to restrict the lateral movement of the trailer [4]. Equal-i-zer employs a combination of the rigid trailer attachments and friction sway control [5]. The limitations of these systems have been well documented [6]. Most of the parameters that affect the lateral stability of car-trailer systems at high speeds may be significantly varied under different operating conditions. These important parameters include the weight distribution and the tire cornering stiffness. Due to the varied operating conditions, the stability of a car-trailer system cannot be guaranteed with a passive mechanism.

To address this problem, various active control methods have been proposed. Hac et al. [7] examine stability of a car-trailer system with an active trailer brake control of the towing unit. Sharp and Fernandez [8] investigate the effects of active trailer braking. The active rear wheel steering of a towing unit has been investigated by Nagai and Kageyama [9]. Minaker and Maiorana [10] study a variable geometry approach (VGA). The essence of this method is to actively control the lateral displacement of the car-trailer hitch in order to improve the high-speed stability of the vehicle system. He et al. [11] have evaluated various active control strategies for improving the lateral stability of car-trailer systems.

This paper presents a new Active Trailer Braking (ATB) controller for improving the lateral stability of the car-trailer systems. An ATB controller, based on the linear quadratic regular (LQR) technique [12-13], is designed for a car-trailer system using a linear vehicle model with 3 Degrees Of Freedom (DOF). In order to examine the performance of the ATB controller, a single lane-change maneuver is simulated and the resulting dynamic responses are compared with those obtained for a baseline design. Through the benchmark investigation, the features of the controller are disclosed.

The paper is organized as follows: Section 2 introduces the vehicle system modeling; the design of the ATB controller is described in section 3 and the numerical simulation results are presented in section 4; finally, conclusions are drawn in section 5.

2. Vehicle System Modeling

2.1 Vehicle Model

For the purpose of the ATB controller design, a 3 DOF linear vehicle model is generated to represent the car-trailer system. The three motions considered here are: (1) the car lateral speed, V; (2) the car yaw rate, r; and (3) the articulation angle between the car and the trailer, ψ. The 3 DOF vehicle model is shown schematically in Fig. 1.

The governing equations of motion of the vehicle model are

$$m_1(\dot{U} - Vr) = -X_1\cos\delta - X_2 + X \tag{1}$$

$$m_1(\dot{V} + Ur) = f_1 + f_2 + X_1\sin\delta - Y \tag{2}$$

$$I_1\dot{r} = af_1 - bf_2 + aX_1\sin\delta + dY \tag{3}$$

The equations of motions of the trailer are written as

$$m_2(\dot{U}' - V'r') = -X_3 - Y\sin\psi - X\cos\psi \tag{4}$$

$$m_2(\dot{V}' + U'r') = f_3 - X\sin\psi + Y\cos\psi \tag{5}$$

$$I_2\dot{r}' = hf_3 - e(X\sin\psi - Y\cos\psi) + \Delta M \tag{6}$$

Since the towing and trailing units are interconnected at the articulation joint, the velocities and accelerations at that point expressed in the coordinate systems as fixed with the car and the trailer must be equal, respectively. This allows the trailer equations to be written in terms of the car fixed coordinate system. Based on the following assumptions, the equations are linearized: (1) the forward speed U is assumed constant and Eqs. (1) and (4) are ignored; (2) the small angle approximations are used, cost ψ = 1, sin ψ = ψ; (3) all the products of variables are ignored; and (4) for the zero initial conditions,

$$\dot{\psi} = r - r' \tag{7}$$

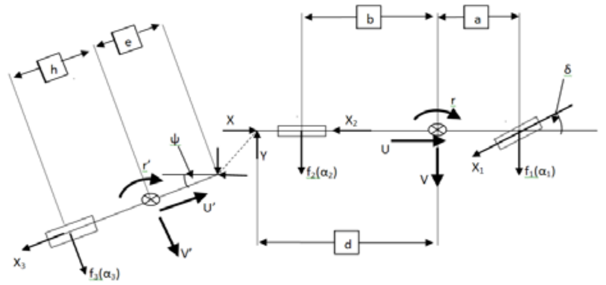

Fig. 1 Schematic representation of the 3 DOF vehicle model.

The linearized equations of motion can be written in the state space form as

$$M\{\dot{X}\}+D\{X\}+Cu+F\delta \tag{8}$$

where the state variable vector is defined as

$$\{X\}=\{V \quad r \quad \dot{\psi} \quad \psi\} \tag{9}$$

and the control variable vector is defined as

$$u=\Delta M \tag{10}$$

In Eq. (8), δ is the car front axle steering angle, the matrices M, D, C and F are listed in Appendix. The primary parameters of the car-trailer system are listed in Table 1.

2.2 Single Lane-Change Maneuver Emulated

To examine the dynamic responses of the car-trailer system in a single lane-change maneuver, the car front wheel steering angle undergoes the following time dependent function:

$$\delta = 0.03\sin((t-0.25)\cdot\pi) \tag{11}$$

In the single lane-change maneuver, the vehicle forward speed maintains at 80 km/h and the car's front wheel steering angle input δ follows the function indicated in Eq. (11), which is shown in Fig. 2. With the simulated maneuver, the vehicle system's dynamic responses can be achieved.

3. Design of ATB Controller

To improve the lateral stability of the car-trailer system, an ATB control system is proposed as shown in Fig. 3. The essential concept of this system is to control the trailer yaw moment through the trailer differential braking. As shown in Fig. 3, four sensors are employed to collect the vehicle state variables, including the car lateral speed, yaw rate, articulation angle, and the time rate of change of the articulation angle. The sensor information will be sent to the controller for manipulating the trailer braking system to produce the trailer yaw moment through differential braking control. Then, the yaw moment will be sent to the car-trailer model. The resulting yaw moment may restrict the unstable motion modes, such as the jack-knifing, trailer swing, and rollover.

Table 1 Primary parameters of the car-trailer system.

Parameter	Symbol	Value
Car mass	m_1	2200 kg
Car yaw inertia	I_1	2000 kg·m^2
Car dimension	a	1.5 m
Car dimension	b	1.7 m
Car dimension	d	2.9 m
Trailer mass	m_2	2000 kg
Trailer yaw inertia	I_2	3000 kg·m^2
Trailer dimension	e	6 m
Trailer dimension	h	0 m
Front tire cornering stiffness	C_1	-80000 Nm/rad
Rear tire cornering stiffness	C_2	-80000 Nm/rad
Trailer tire cornering stiffness	C_3	-80000 Nm/rad

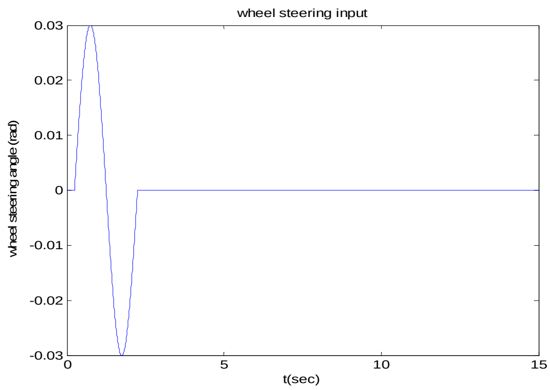

Fig. 2 Steering angle input for the car front wheels in the single lane-change maneuver.

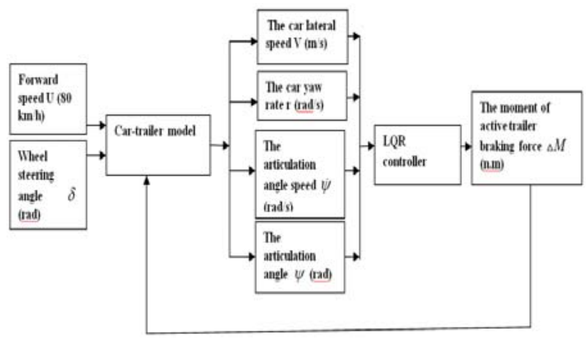

Fig. 3 Proposed ATB control system.

The ATB controller is developed using the LQR technique, which is an optimization problem, and the goal is to minimize the performance index:

$$J = \int_0^\infty \left[q_1 \left(\dot{V} + Ur \right)^2 + q_2 \left(\dot{V}' + U'r' \right)^2 + q_3 \Delta M^2 \right] dt \quad (12)$$

subject to Eq. (8). By solving the algebraic Riccati equation, the solution of the optimization problem is the control vector of the form:

$$u = -\{K\}\{X\}^T \quad (13)$$

where $\{K\}$ is the control gain matrix, and $\{X\}^T$ and u are the state and control variable vectors defined by Eqs. (9)-(10), respectively. In Eq. (12), q_1, q_2, and q_3 are the weighting factors that impose penalties upon the magnitude and duration of the lateral acceleration at the car Center of Gravity (CG), the lateral acceleration at the trailer CG, and the active trailer yaw moment ΔM. Note that the third term on the right hand side of Eq. (12) represents the energy consumption of the ATB control system.

As shown in Eq. (12), by coordinating the relationship between the lateral accelerations at the car CG and the trailer CG, the articulation angle between the car and trailer and the roll angles of car and trailer bodies will be under controlled. Thus, the dangerous jack-knifing and trailer swing may be prevented altogether. Moreover, both the magnitudes of the lateral accelerations at the car CG and the trailer CG are to be minimized. Thus, the rollover stability will be enhanced. The above design considerations will be justified in the next section.

4. Simulation Results and Discussion

4.1 Numerical Simulation

The vehicle system model introduced in section 2, and the ATB controller designed in section 3 are jointly constructed and integrated in Matlab©/Simulink© as shown in Fig. 4.

Using the vehicle system parameters listed in Table 1, with the vehicle system model constructed in Simulink shown in Fig. 4, the numerical simulations for the single lane-change maneuver can be conducted.

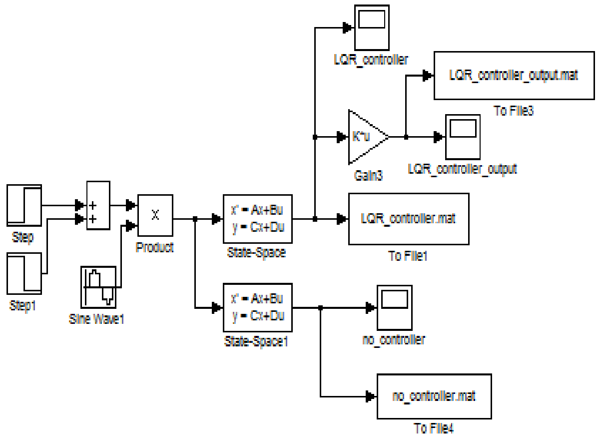

Fig. 4 Integration of the car-trailer model with the ATB controller.

For the purpose of comparison, the numerical simulations based on both the car-trailer model with and without the ATB controller have been performed. The respective numerical simulation results are presented and discussed in the following subsection.

4.2 Results and Discussion

In order to examine the performance of the ATB controller, the selected numerical results based on the simulated single lane-change maneuver are illustrated and discussed. The simulation results for the car-trailer system with the ATB controller are shown in Figs. 5-9. For the purpose of comparison, the corresponding simulation results for the baseline design without the ATB controller are also presented in the figures.

The time history diagrams of the car's yaw rate for both the designs with and without the ATB controller are shown in Fig. 5. For the baseline design, the yaw rate oscillation is damped out after 12 seconds. The maximum peak value of the oscillation is 0.24 rad/s. For the design with the ATB controller, the car yaw rate oscillation is damped out after only 4 seconds, a reduction of 8 seconds from the corresponding baseline value of 12 seconds. The maximum peak value of the oscillation for the design with the ATB controller is only 0.08 rad/s, decreasing 67% from the baseline value of 0.24 rad/s. The results shown in Fig. 5 indicate that the ATB controller installed on the trailer has a significant dynamic impact on the leading unit.

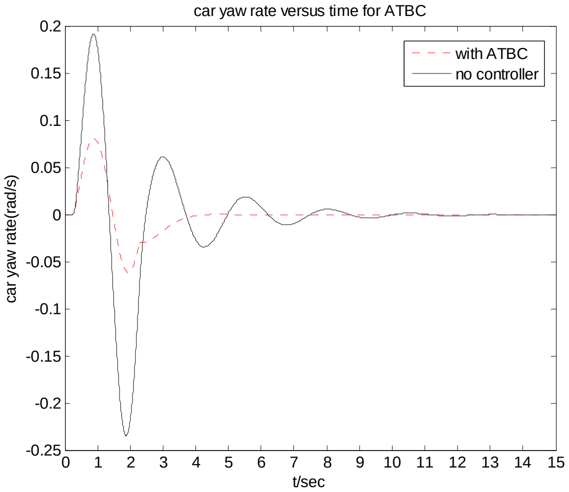

Fig. 5 Time history of car yaw rate for the designs with and without the ATB controller.

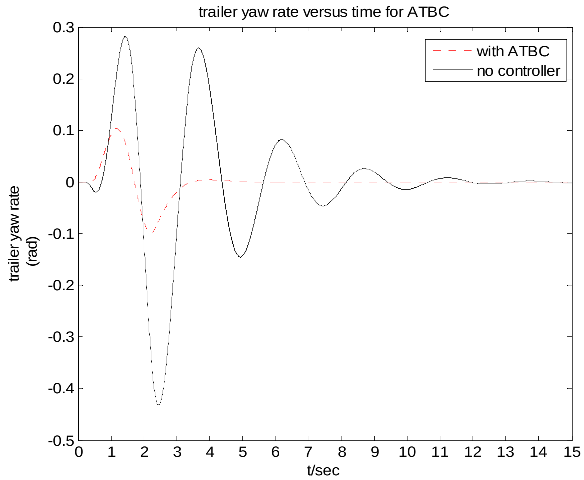

Fig. 6 Time history of trailer yaw rate for the designs with and without the ATB controller.

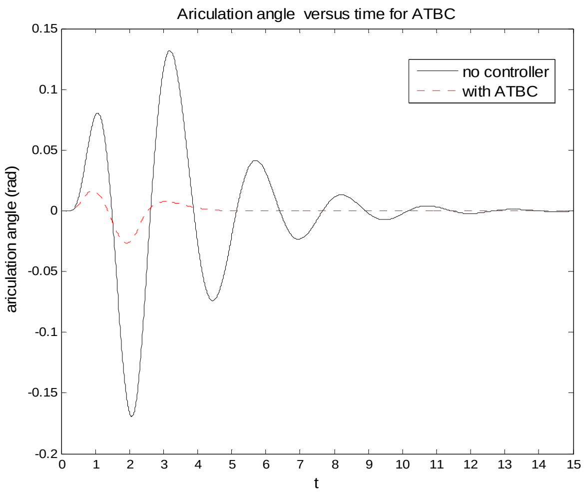

Fig. 7 Time history of articulation angle between the car and the trailer for the designs with and without the ATB controller.

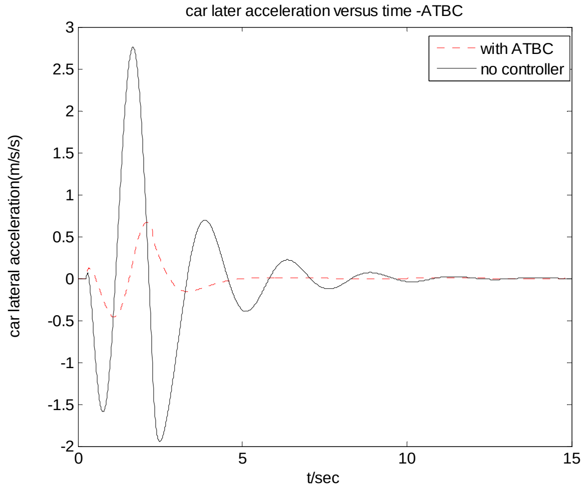

Fig. 8 Car lateral acceleration versus time for the car-trailer system with and without the ABT controller.

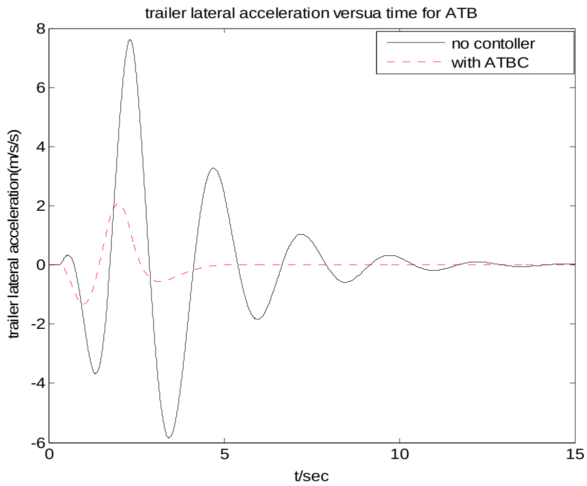

Fig. 9 Trailer lateral acceleration versus time for the car-trailer system with and without the ABT controller.

The time history diagrams of the trailer yaw rate for both designs with and without the ATB controller are illustrated in Fig. 6. In the baseline design, the maximum peak and the settling time of the yaw rate oscillation take the values of 0.45 rad/s and 15 seconds, respectively. In the design with the ATB controller, the maximum peak value is 0.1 rad/s, reducing to 77.8% from the baseline value; the settling time is 4 seconds, decreasing 11 seconds from the baseline value of 15 seconds. The ATB controller directly contributes the improvement of the trailer yaw rate response.

Fig. 7 illustrates the time history diagrams of the articulation angle between the car and trailer in both designs with and without the ATB controller. In the case of the ATB controller, the maximum peak value of the articulation angle variation is 0.027 rad, reducing 85% from the baseline value of 0.18 rad; the settling time of the angle oscillation is 4 seconds, decreasing 10 seconds from the baseline value of 14 seconds.

Fig. 8 offers the simulation results in terms of the car lateral acceleration versus time for the designs with and without ATB controller. In the case of ATB controller, the maximum peak value of the car acceleration variation is 0.65 m/s^2, reducing 78.8% from the baseline value of 2.8 m/s^2; the settling time of the car lateral acceleration oscillation is 5 seconds, decreasing 6.5 seconds from the baseline value of 11.5 seconds. With a smaller lateral acceleration, the car will have less chance to undergo the rollover. Thus, the ATB controller will contribute to the roll stability improvement of the car-trailer system.

The relationship between the trailer's lateral acceleration and time for both designs with and without the ATB controller are illustrated in Fig. 9. Compared with the baseline design, the system with the ATB controller has a better trailer lateral acceleration response: (1) the maximum trailer acceleration peak value is 2.07 m/s^2, reducing 72.73% from the baseline value of 7.59 m/s^2; (2) the settling time of the trailer lateral acceleration oscillation is 5 seconds, decreasing 10 seconds from the baseline value of 15 seconds. It is expected that for the baseline design, the trailer may rollover because the trailer lateral acceleration already reaches 7.59 m/s^2, i.e., 0.77g, which is higher than the rollover threshold of 0.6g for the regular car-trailer systems [3].

The yaw moment resulting from the ATB control is shown in Fig. 10. In the simulated single lane-change maneuver, the maximum control moment of 6300 Nm is required. This yaw moment resulting from the differential braking control will reject the disturbance torque or force that may introduce the unstable motion modes, including the jack-knifing, trailer swing, and the vehicle rollover.

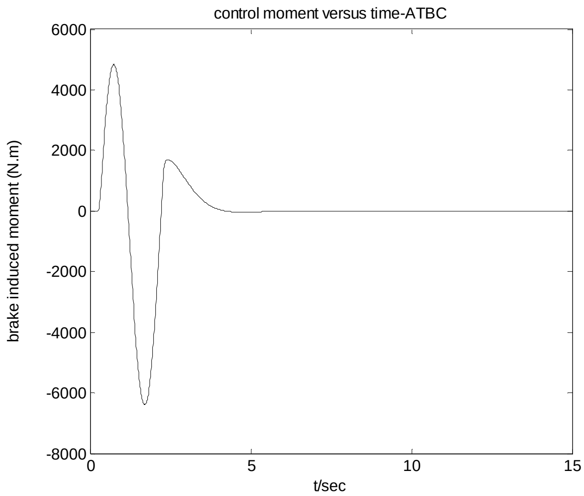

Fig. 10 Control yaw moment versus time for the car-trailer system with the ATB controller.

To quantitatively analyze the car-trailer system lateral stability for the designs with and without the ATB controller, the dynamic responses in the single lane-change maneuver are summarized in Table 2.

As discussed above, compared with the baseline design, the system with the ATB controller has better performance in terms of vehicle dynamic responses in the simulated single lane-change maneuver. As shown in Table 2, in terms of car lateral acceleration, car yaw rate, articulation angle, trailer yaw rate, and trailer lateral acceleration, the system with the ATB controller has much smaller peak values and less settling times than those of the baseline design.

5. Conclusions

This paper presents an Active Trailer Braking (ATB) controller for car-trailer systems in order to improve the lateral stability at high speeds. The controller is derived with a 3 Degrees Of Freedom (DOF) yaw/plan vehicle model using the Linear Quadratic Regulator (LQR) technique. In the controller design, the car lateral acceleration, the trailer lateral acceleration and the control moment derived from the ATB control are coordinated and manipulated in such a way that the unstable motion modes of the vehicle, including the jack-knifing, trailer swing, and rollover, could be prevented.

Table 2 Car-trailer dynamic responses in the simulated single lane change maneuver.

Design cases	Max. car lateral acceleration (m/s2)	Settling time (s)
Baseline design	2.8	16.5
ATB controller	0.65	5

Design cases	Max. car yaw rate (rad/s)	Settling time (s)
Baseline design	0.24	12
ATB controller	0.08	5

Design cases	Max. trailer lateral acceleration (m/s^2)	Settling time (s)
Baseline design	7.59	15
ATB controller	2.07	4

Design cases	Max. trailer yaw rate (rad/s)	Settling time (s)
Baseline design	0.45	15
ATB controller	0.1	4

Design cases	Max. articulation angel (rad/s)	Settling time (s)
Baseline design	0.18	14
ATB controller	0.027	4

To examine the performance of the controller, a single lane-change maneuver has been simulated and the numerical results are compared with those of the baseline design without the controller. Simulation results indicate that compared with the baseline design, the system with the ATB controller has enhanced lateral stability at high speeds. With respect to the baseline design, the enhanced stability of the system with the ATB controller is reflected in terms of much less magnitudes and shorter settling times in the dynamic responses of car lateral acceleration, car yaw rate, trailer lateral acceleration, trailer yaw rate, and articulation angle between the car and the trailer. The control yaw moment derived from the trailer differential braking control contributes to the improvement of lateral stability of the car-trailer system. In the future research, the ATB controller design will be improved considering various operating conditions, such as the variation of vehicle forward speeds and trailer payloads.

Acknowledgments

The financial support of this research received from the Natural Sciences and Engineering Research Council of Canada (NSERC) and the Canada Foundation for Innovation (CFI) is acknowledged.

References

[1] A. Clay, J. Montufar, D. Middleton, Operation of long semi-trailers in the United States, Transportation Research Record 1833 (2003) 79-86.

[2] F. Vlk, Handling performance of truck-trailer vehicles: A state-of-art survey, Int. J. of Vehicle Design 6 (3) (1985) 323-361.

[3] C. Winkler, Rollover of heavy commercial vehicles, UMTRI Research Review 31 (2000) 1-17.

[4] Hensley, The Secret of the Hensley Arrow, http://www.hensleymfg.com/ how_it_works.shtml.

[5] Equal-i-zer, 4-Point Sway Control, http://www.equalizerhitch.com/productinfo/4point_sway_control.pp.

[6] R.S. Sharp, M.A.A. Fernandez, Car-caravan snaking: Part 1. The influence of pintle pin friction, MS Thesis, School of Engineering, Cranfield University, Bedford, 2001.

[7] A. Hac, D. Fulk, H. Chen, Stability and control considerations of vehicle-trailer combination, SAE Int. J. Passeng. Cars - Mech. Syst. 1 (1) (2009) 925-937.

[8] R.S. Sharp, M.A.A. Fernandez, Car-caravan snaking: Part 2. Active caravan braking, MS Thesis, School of Engineering, Cranfield University, Bedford, 2001.

[9] R. Nagai, I. Kageyama, Stabilization of passenger car-caravan combination using four wheel steering control, Vehicle System Dynamics 24 (4) (1995) 313-327.

[10] B.P. Minaker, J. Maiorana, Active control of trailer dynamics using variable geometry, in: Proceedings of the CSME Forum 2004, Canada, June 1-4, 2004.

[11] R. Shamim, M. Islam, Y. He, A comparative study of active control strategies for improving lateral stability of car trailer systems, SAE Technical Paper, doi: 10.4271/2011-01-0959.

[12] J. Hespanha, Linear Systems Theory, Princeton University Press, USA, 2009.

[13] A. Bryson, Y. Ho, Applied Optimal Control: Optimization, Estimation and Control, Wiley, New York, 1975.

Appendix

$$M = \begin{bmatrix} m_1 + m_2 & -m_2(d+e) & m_2 e & 0 \\ -m_2 d & I_1 + m_2 d(d+e) & -m_2 ed & 0 \\ -m_2 e & I_2 + m_2 e(d+e) & -I_2 - m_2 e^2 & 0 \\ 0 & 0 & 0 & 1 \end{bmatrix}$$

$$C = \begin{bmatrix} 0 \\ 0 \\ -1 \\ 0 \end{bmatrix}$$

$$D = \frac{1}{\mu} \times \begin{bmatrix} c_1 + c_2 + c_3 & c_1 a - c_2 b - c_3(d+e+h) - (m_1 + m_2)\mu^2 & c_3(h+e) & c_3 \mu \\ c_1 a - c_2 b - c_3 d & c_1 a^2 + c_2 b^2 + c_3 d(d+e+h) + m_2 d \mu^2 & -c_3 d(e+h) & -c_3 d \mu \\ -c_3(h+e) & c_3(d+h+e)*(h+e) + m_2 e \mu^2 & -c_3(h+e)^2 & -c_3(h+e)\mu \\ 0 & 0 & \mu & 0 \end{bmatrix} \Delta M$$

$$F = \begin{bmatrix} -c_1 \\ -c_1 a \\ 0 \\ 0 \end{bmatrix}$$